DOI: 10.1002/chem.200802160

Furazan-Functionalized Tetrazolate-Based Salts: A New Family of Insensitive Energetic Materials

Ruihu Wang,[a] Yong Guo,[b] Zhuo Zeng,[b] Brendan Twamley,[b] and Jean′ne M. Shreeve*[b]

Abstract: Furazan-functionalized tetrazolate-based energetic salts (**1**–**13**) were prepared by direct treatment of neutral 4-amino-3-(5-tetrazole)furazan and a Lewis base or by simple metathesis reactions of its barium salt formed in situ with the corresponding sulfate salts in aqueous solution. Key physical properties, such as melting point, thermal stability, density, hypergolicity, and sensitivity to shock, were measured. The relationship between their structures and these properties was determined. Most of salts exhibit better thermal stability than their 5-nitrotetrazolate and 5-nitraminotetrazolate analogues as well as other furazan-based salts. The structures of representative aminoguanidinium (**4**), carbonic hydrazylhydrazidinium (**9**), and 1,4-dimethyl-5-aminotetrazolium salts (**13**) were further confirmed by single-crystal X-ray analysis. Their densities, heats of formation, detonation pressures and velocities, and specific impulses were calculated. All of the salts possess high positive heats of formation. The effect of the furazan ring on these physicochemical properties was examined and discussed.

Keywords: ab initio calculations · energetic salts · explosives · furazan · nitrogen heterocycles

Introduction

High-nitrogen heterocyclic systems have long been recognized as one class of useful and promising structures for the design and synthesis of high-energy density materials (HEDMs).[1,2] A number of heterocycle-based energetic compounds were reported and were extensively used as high explosives and ingredients of propellants. Of these, the furazan group is an efficient fragment to enhance the performance of HEDMs, many azide, nitro- and nitramine-functionalized mono-furazan compounds,[3] as well as the chained furazans,[4] macrocyclic furazans,[5] and ring-fused furazans[6] bridged by oxy, azo, and azoxy groups have been investigated.[7] Most of them show low vulnerability, higher density, positive heat of formation, and a high percentage of nitrogen content. Moreover, furazan derivatives have been reported to exhibit a wide spectrum of biological properties, such as antimicrobial, antituberculous, spasmolytic, and muscle relaxant activity. Their agrochemical application as herbicides, plant-growth regulators, and pesticides have also been described, and thus they have a potential application as biologically active energetic materials.[8]

Recently, considerable efforts have focused on studying nitrogen-containing heterocyclic energetic salts with higher performance and/or decreased sensitivity as well as environmental compatibility.[1e,9–14] Salt-based energetic materials often possess advantages over nonionic molecules since these salts tend to exhibit lower vapor pressures and higher thermal stability than their atomically similar nonionic analogues. Many organic cations and anions deriving from imidazole,[11b,c] triazole,[1e,9,13c] and tetrazole[12,14] have been reported, their properties are readily tuned and optimized through independent variation and modification of the cationic and/or anionic components. However, the absence of an acidic proton in the furazan ring makes it impossible to serve as Brønsted acid and to pair with Lewis base; in addition, the electron-withdrawing character of the furazan ring

---

[a] Dr. R. Wang
State Key Laboratory of Structural Chemistry
Fujian Institute of Research on the Structure of Matter
Chinese Academy of Science,
Fuzhou, Fujian 350002 (China)

[b] Dr. Y. Guo, Dr. Z. Zeng, Dr. B. Twamley, Prof. Dr. J. M. Shreeve
Department of Chemistry
University of Idaho
Moscow, Idaho, 83844-2343 (USA)
Fax: (+1) 208-885-9146
E-mail: jshreeve@uidaho.edu

Supporting information for this article is available on the WWW under http://dx.doi.org/10.1002/chem.200802160.

hinders protonation or direct substitution of the nitrogen atoms in the ring,[7,15] thus, it could not act as a cation in energetic salts. But the combination of the furazan ring with other energetic groups or backbones containing acidic protons may serve as the anion after deprotonation. The primary nitramine-functionalized furazan-based compounds, 3-nitramino-4-nitrofurazan[16] and 3,6-bis(4-nitroamino-1,2,5-oxadiazol-3-yl)-1,4,2,5-dioxadiazine[17] were synthesized, and were used as energetic anions, but most of organic salts possess lower thermal stability. Further development of energetic materials requires the optimal tradeoff in energy content, safety, cost, and environmental impact. It is expected that the combination of the furazan fragment with other energetic backbones containing acidic protons into one molecule would lead to new energetic salts, which would possess positive properties of both classes. However, this type of energetic salt has not been reported.

Tetrazole derivatives are another class of interesting HEDMs owing to the high-nitrogen content, ready availability, high positive heat of formation, and good thermal stability deriving from its aromaticity.[12,14] Among them, 5-nitrotetrazolium-based salts were extensively investigated and show promising energetic performance.[12g,14c,e] In this context, theoretical modeling studies show that when a nitro group is displaced by a furazan group in energetic compounds, the density, heat of formation, and detonation velocity can increase by about 0.06–0.08 $g\,cm^{-3}$, 200 $kJ\,mol^{-1}$, and 300 $m\,s^{-1}$, respectively.[18] For example, the calculated heat of formation of the 3-aminofurazan group (200.1 $kJ\,mol^{-1}$) is much higher than that of NH_2NO_2 (-6.1 $kJ\,mol^{-1}$). Thus, it would be valuable to introduce furazan into tetrazole compounds since tetrazole is readily deprotonated and converted to the corresponding anions. In our program in which we seek more powerful, less sensitive energetic salts,[1e, 11, 12] we have reported a series of triazolyl- and triazolium-functionalized unsymmetrical energetic salts and they showed some novel properties that could not be obtained through mono-energetic fragments owing to the synergistic effect of two energetic rings.[11c] As a continuation of our study of energetic salts containing different energetic backbones, we now report the syntheses and characterization of a series of furazan-functionalized tetrazolium-based energetic salts. The choice of nitrogen-rich heterocyclic and non-heterocyclic monocations and dications was made to establish the broad relative potential to comprehensively evaluate their performance.

Results and Discussion

The synthetic pathway to all of the new energetic salts is depicted in Scheme 1. 4-Amino-3-(5-tetrazolyl)furazan (HAFT) was easily synthesized through the reaction of malononitrile, sodium nitrite, and hydroxylamine,[19a] followed by oxidation with PbO_2, and cycloaddition with NaN_3.[19b,c] Direct reactions of HAFT with ammonia and 1-methylimidazole resulted in the formation of salts **1** and **10**, respectively (see Table 1 for structures), but the similar reactions with guanidine carbonate and aminoguanidine bicarbonate failed to generate corresponding salts, which suggests the low acidity of HAFT. An alternative synthesis of the energetic salts is based on metathesis reactions of the silver and barium salts with halides and sulfates, respectively; the driving force of these reactions is the formation of silver halide and barium sulfate, which have a very low solubility in water and can be easily removed by simple filtration. The treatment of HAFT with an equivalent amount of aqueous sodium hydroxide, and then with an equivalent of silver nitrate gave rise to Ag(AFT) as a colorless solid, but the poor solubility of this silver salt in common solvents limits its use. Encouragingly, its barium salt has good solubility in water, MeOH, and EtOH. Thus, energetic salts **2**–**9** were readily synthesized by metathesis reactions of $Ba(AFT)_2$ formed in situ with corresponding sulfate salts. It should be mentioned that the reactions of $Ba(AFT)_2$ with an equivalent amount of dicationic carbonic dihydrazidinium sulfate and biguanidinium sulfate gave rise to the monocationic salts **8** and **9**, respectively, which was confirmed by elemental analysis and the crystal structure of **9** (vide infra). With similar protocols, the heterocycle-based energetic salts **11**–**13** were prepared through one-pot reactions of iodide salts, Ag_2SO_4, HAFT, and $Ba(OH)_2$.

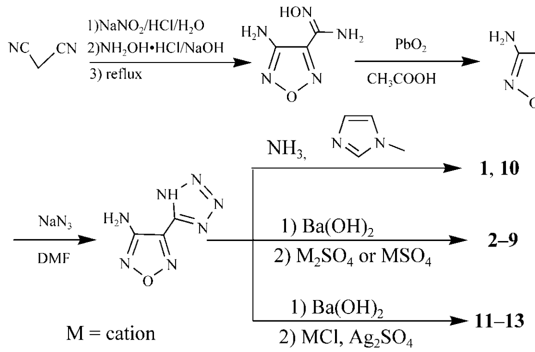

Scheme 1.

All of the energetic salts are stable in air and may be stored for a long period. They are soluble in MeCN, MeOH, H_2O, and DMF, while insoluble in lower polar solvents, such as hexane, diethyl ether, dichloromethane, and ethyl acetate. Their structures were confirmed by ^1H, ^{13}C NMR, and IR spectroscopy, and elemental analyses. The ^1H NMR spectrum of HAFT shows a rapid exchange with the protons in $[D_6]$DMSO, and only a broad signal together with water at $\delta = 4.19$ ppm is observed. However, salts **1**–**13** exhibit a sharp single peak around $\delta = 6.51$ ppm for the amine group of AFT. In ^{13}C NMR spectra, the chemical shift of the furazan carbon bonded to NH_2 in the salts is similar to that of HAFT ($\delta = 155.8$ ppm); the chemical shifts of the other furazan carbon and tetrazolate carbon are around $\delta = 140.3$ and 151.0 ppm, respectively, which are obvious downfield shifts compared with those of their precursor HAFT ($\delta =$ 136.6 and 147.9 ppm). It should be mentioned that the

^{13}C NMR resonance of the tetrazolate carbon is at a higher field than that of the 5-nitrotetrazolate salts ($\delta \approx 169$ ppm)[12g,14c,e] and 5-nitraminotetrazolate ($\delta \approx 159$ ppm),[12g,h,14b] which suggests the lower electron-withdrawing ability of furazan than that of nitro and nitramino substituents. In salt **2**, there appears to be a fast proton exchange since a single peak at $\delta = 6.52$ ppm in its ^{1}H NMR spectrum is found as one only signal together with water in [D$_6$]DMSO.

Physical properties of the energetic salts: Phase transition temperature (midpoint of melting point) and thermal stability of the salts **1**–**13** were determined by differential scanning calorimetry (DSC) and thermogravimetric analysis (TGA), respectively. As shown in Table 1, ammonium salt **1**, possesses the highest melting point ($T_m = 278$ °C) and thermal degradation temperature ($T_d = 289$ °C). For guanidinium-derivatized salts **3**–**9**, melting points and thermal degradation temperatures are in the range of 149–225 and 213–262 °C, respectively, which are comparable with that of commonly used explosive RDX ($T_m = 204$, $T_d = 230$ °C). The lower melting point of the diaminoguanidinium salt **5** (149 °C) is surprising. For the *N*-carbamoylguanidinium salt **7** in addition to an endotherm at 211 °C, its DSC curve shows another smaller endotherm at 103 °C, corresponding to the loss of water. This was further shown by 5.25 % weight loss from 74 to 118 °C (calcd, 6.59 %) in its TGA curve. The melting point of **11** ($T_m = 55$ °C) is below 100 °C; thus, **11** is classifiable as an ionic liquid.[20] It should be pointed out that the 1,4-dimethyl-5-aminotetrazolium salt **13** has a higher melting point and better thermal stability than the other heterocycle-based salts **10**–**12**, which most likely can be ascribed to the more extensive hydrogen bonding interactions between its cation and anion, as observed in its crystal structure (vide infra). As such, the absent or weak hydrogen bonds in **12** result in the lowest thermal stability in these salts ($T_d = 170$ °C). When comparing with nitrotetrazolate[12g,14c,e] and 5-nitraminotetrazolate[12g,h,14b] analogues, most of the salts possess lower melting pointing and higher thermal stability.

Table 1. Physical properties of energetic salts.

Compd	Cation	T_m[a] [°C]	T_d[b] [°C]	d_{calcd}[c] [g cm^{-3}]	d_{meas}[d] [g cm^{-3}]	Oxygen balance[e]
1	$NH_4^{\oplus}$	278	289	1.61	1.62	−75.2
2	$H_2N{-}NH_3^{\oplus}$	161	197	1.60	1.60	−73.5
3	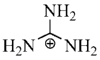	181	262	1.53	1.50	−83.0
4	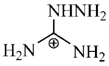	189	257	1.55	1.55	−81.0
5	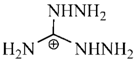	149	228	1.57	1.54	−79.3
6	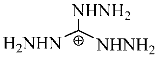	207	216	1.60	1.62	−77.8
7	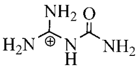	211	213	1.59[f] (1.63)[f,g]	1.64 (1.68)[h]	−78.4
8	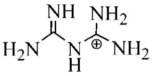	225	251	1.58[f]	1.77	−88.1
9	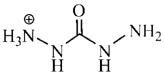	162	199	1.66	1.68	−69.1
10		125	262	1.48	1.45	−119.0
11	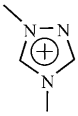	55	204	1.47 (1.48[g])	1.46 (1.47[h])	−115.1
12	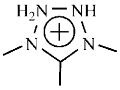	109	170	1.47	1.44	−111.6
13	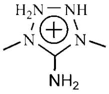	205	212	1.51	1.51	−96.2

[a] Melting point. [b] Thermal degradation. [c] Calculated density. [d] Measured density. [e] Oxygen balance (OB) is an index of the deficiency or excess of oxygen in a compound required to convert all C into CO_2 and all H into H_2O, for a compound with the molecular formula of $C_aH_bN_cO_d$, OB (%) $= 1600[(d-2a-b/2)/M_W]$. [f] Volume of the salts was corrected by −8 Å for strong hydrogen bonds. [g] Calculated density without water molecule. [h] Density was corrected by −25 Å for volume of each water molecule.

It is well known that hydrogen-bonding interactions not only can help stabilize energetic compounds substantially, but also can increase their density markedly. Density is one of the most important factors that determine the performances of energetic compounds. The densities of the non-heterocycle-based salts **1**–**9** and heterocycle-based salts **10**–**13** are in the range of 1.50–1.77 g cm^{-3} and 1.44–1.51 g cm^{-3}, respectively. The former is lower than those of their nitrotetrazolate analogues[12g,14c,e] since the salts containing NO_2 and NH_2 are more inclined to form strong hydrogen bonds. The densities were also estimated according to our tabulated volume parameters,[21] which agreed reasonably with the experimental values within 5 % deviation with the exception of **8**. As expected, the measured densities of **4**, **9**, and **13** are slightly lower than those from X-ray crystal structures (vide infra), since the molecules in the single-crystal state are most efficiently packed.

Oxygen balance (OB) is used to indicate the degree to which a compound can be oxidized. Owing to the presence of two carbon atoms in the furazan ring and the absence of oxygen atoms in the salts, all of them possess negative OB and are in the range from −69.1 to −119.0, which are comparable with that of TNT (−74).

When each of the salts was added to liquid NO_2 or 100 % nitric acid, no ignition was observed, which indicates they have no hypergolic properties.[22]

Impact sensitivities of the salts were tested with a BAM Fallhammer and about 20 mg samples were used. When a 10 kg mass was dropped from 40 cm, no explosion occurred, suggesting that the salts are insensitive to shock.[14a]

Heats of formation are another important parameter to evaluate the performances of energetic salts. This property of the salts can be calculated with good accuracy (including the heat of formation of the cation and anion, and lattice energy of salts).[23] The heat of formation of the AFT anion was calculated based on the isodesmic reaction given in Scheme 2, in which the heat of formation of furazan was calculated by using the G2 method (196.71 kJ mol^{-1}). The heat of formation the AFT anion (306.7) kJ mol^{-1} is much higher than that of aminotetrazolate (183.8 kJ mol^{-1}), nitrotetrazolate (112.8 kJ mol^{-1}), and 5-nitraminotetrazolate (9.8 kJ mol^{-1}),[23] thus, their salts exhibit much higher heats of formation than their aminotetrazolate,[14f,23] 5-nitrotetrazolate[12g,14c,e] and 5-nitraminotetrazolate[12h,14b] analogues. For example, the heat of formation of hydrazinium, guanidinium, aminoguanidinium, and diaminoguanidinium salts are 561.4, 393.6, 489.6, and 599.9 kJ mol^{-1}, respectively; the heats of formation of the corresponding nitrotetrazolate salts are 343.7, 191.2, 307.9, and 437.2 kJ mol^{-1}, respectively.[14e] As shown in Table 2, the heats of formation of the salts **1**–**13** fall in the range from 177.2 to 730.1 kJ mol^{-1}, in which *N*-carbamoylguanidinium and 1,4-dimethyl-5-aminotetrazolium salts possess the lowest and highest heats of formation, respectively. As anticipated, the effect of guanidinium-derivatized cation and heterocyclic cation on the heat of formation is in the following order: triaminoguanidinium > diaminoguanidinium > aminoguanidinium > guanidylguanidinium > guanidinium > *N*-carbamoylguanidinium and 1,4-dimethyl-5-aminotetrazolium > 1,4,5-trimethyltetrazolium > 1,4-dimethyltriazolium > 1-methylimidazolium, respectively.

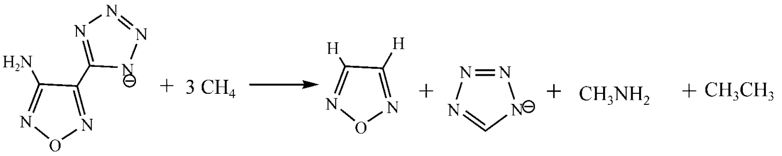

Scheme 2.

Table 2. Thermochemical results of energetic salts.

Compd	$\Delta_f H_{cation}$[a] [kJ mol^{-1}]	$\Delta_f H_{lat}$[b] [kJ mol^{-1}]	$\Delta_f H_{salt}$[c] [kJ mol^{-1}]	$\Delta_f H_{salt}$[d] [kJ g^{-1}]	P[e]	νD[f]	I_{sp}[g]
1	626.4	521.6	411.5	2.42	22.9	8075	214.6
2	770.0	515.3	561.4	3.03	24.8	8338	229.7
3	575.9	489.0	393.6	1.85	18.5	7640	194.2
4	667.4	484.5	489.6	2.16	20.4	7747	203.4
5	769.0	475.8	599.9	2.48	21.6	7932	212.5
6	871.5	474.6	703.5	2.74	25.4	8544	219.5
7[h]	350.6	480.1	177.2	0.69	19.9	7732	182.3
8	620.9	487.1	440.5	1.73	25.9	8673	188.2
9	663.4	486.1	484.0	1.99	25.7	8466	213.0
10	680.6	472.0	515.2	2.19	15.8	7063	195.0
11[h]	756.9	466.2	597.4	2.39	17.5	7372	203.1
12	844.8	457.0	694.5	2.62	17.6	7412	208.1
13	885.5	462.1	730.1	2.74	19.7	7338	212.6

[a] Calculated molar enthalpy of formation of cation. [b] Calculated molar lattice energy (kJ mol^{-1}). [c] Calculated molar enthalpy of formation of salts in kJ mol^{-1}. [d] Calculated molar enthalpy of formation of salts in kJ g^{-1}. [e] Detonation pressures (GPa). [f] Detonation velocities (m s^{-1}). [g] I_{sp} is the specific impulse (seconds) calculated isobarically at 68 atm. [h] Density was corrected by −25 Å for volume of each water molecule.

The energetic performances of salts are characterized by their detonation velocity and pressure, and specific impulse (I_{sp}). These parameters are directly related to density, heat of formation, and oxygen balance of salts. The detonation pressure and velocity (based on the traditional Chapman–Jouget thermodynamic detonation theory) and I_{sp} were obtained by using CHEETAH 5.0.[24] As shown in Table 2, for salts **1**–**13**, the calculated detonation pressures (P) lie, in the range of 15.8–25.9 GPa, which is comparable with that of TNT (2,4,6-trinitrotoluene, 19.53 GPa). The detonation pressures of salts **2** (24.8 GPa), **6** (25.4 GPa), **8** (25.7 GPa), and **9** (25.9 GPa) are higher than that of ADN (ammonium dinitramide, 23.72 GPa). Detonation velocities (D) are found in the range from 7063 m s^{-1} [comparable to TNT, 6881 m s^{-1}] to 8673 m s^{-1} [comparable to TATB (triaminotrinitrobenzene), 8114 m s^{-1} and RDX (cyclotrimethylenetrinitramine), 8977 m s^{-1}]. The range of specific impulse (I_{sp}) in salts **1**–**13** falls in 172.5–229.7 s. Noteworthy, these performances are comparable with those of nitrotetrazolate analogues[12g,14c,e] despite the fact that these salts have lower densities and oxygen balances.

Crystal structures of 4, 9, and 13: Single-crystal X-ray diffraction revealed that compound **4** crystallizes in the monoclinic space group $P2_1/c$ as a racemic twin (Table 3). As shown in Figure 1 a, the asymmetric unit consists of two crystallographically independent AFT anions and two ami-

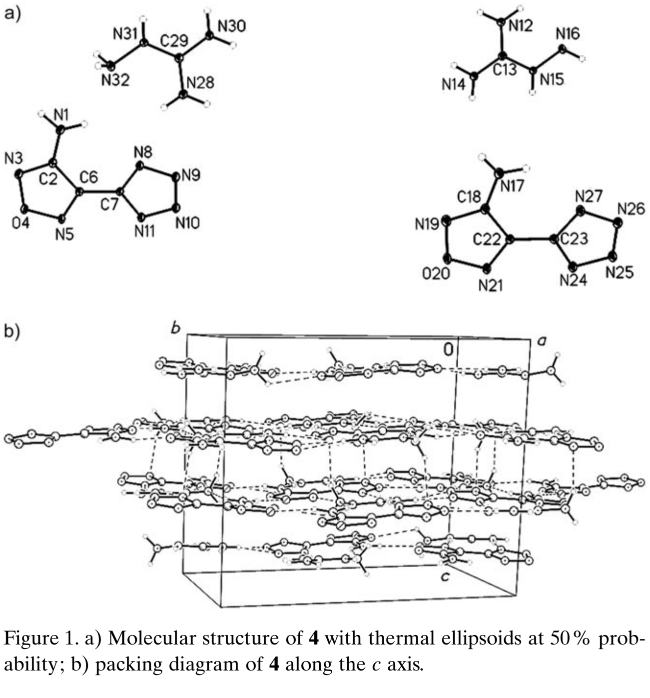

Figure 1. a) Molecular structure of **4** with thermal ellipsoids at 50 % probability; b) packing diagram of **4** along the *c* axis.

Table 3. Crystallographic data for compounds **4**, **9**, and **13**.

	4	**9**	**13**
empirical formula	$C_4H_9N_{11}O$	$C_4H_9N_{11}O_2$	$C_6H_{10}N_{12}O$
fw	227.22	243.22	266.26
crystal size [mm]	0.60×0.05× 0.04	0.84×0.54×0.21	0.54×0.19×0.19
crystal system	monoclinic	monoclinic	orthorhombic
space group	*P*2(1)/*c*	*C*2/*c*	*P*2(1)2(1)2(1)
a [Å]	10.1892(7)	24.9859(7)	5.6426(5)
b [Å]	14.6566(10)	4.3960(1)	11.8331(11)
c [Å]	12.5585(9)	19.6851(6)	17.1998(16)
β [°]	95.380(1)	120.358(1)	
V [Å^3]	1867.2(2)	1865.70(9)	1148.42(18)
Z	8	8	4
T [K]	90(2)	140(2)	90(2)
ρ_{calcd} [g cm^{-3}]	1.617	1.732	1.540
μ [mm^{-1}]	0.128	0.142	0.119
$\lambda(Mo_{K\alpha})$ [Å]	0.71073	0.71073	0.71073
F(000)	944	1008	552
reflections collected	23975	8131	16893
independent reflections	4265	2309	1917
R_{int}	0.0465	0.0174	0.0211
parameters	353	168	212
S on F^2	1.042	1.042	1.067
$R_1(I>2\sigma(I))$[a]	0.0455	0.0330	0.0278
wR_2(all data)[b]	0.1275	0.0905	0.0688
Largest diff. peak and hole [e Å^{-3}]	0.331 and −0.329	0.408 and −0.305	0.326 and −0.158

[a] $R=\Sigma||F_0|-|F||)/\Sigma|F|$. [b] $wR=[\Sigma w(F_0^2-F_c^2)^2/\Sigma w(F_0^2)^2]$.

noguanidinium cations, in which the proton transfer from the tetrazole of HAFT to aminoguanidine is confirmed. In two independent AFT anions, the tetrazolate and furazan are slightly twisted with the dihedral angles between them of 7.8 and 5.0°. The atoms in either tetrazolate or furazan rings are planar with mean deviations from their respective plane of 0.0015, 0.0020, and 0.0023, 0.0030 Å, respectively. The exocyclic amine nitrogen atoms (N1, N17) are out of the furazan plane by 0.0359 and 0.0104 Å, respectively. The atoms of the aminoguanidinium cation are also planar with the mean deviation from the plane being 0.0117 and 0.0327 Å. The C−N bond lengths and the N-C-N bond angles in the cation are in the range 1.317(2)–1.341(2) Å and 117.85(16)–121.28(16)°, respectively, which are typical values for the aminoguanidinium cation.[14e] Since the amino groups in both AFT and aminoguanidinidium are excellent hydrogen-bonding donors, the discrete AFT and aminoguanidinium are linked into a 2D double layer by the hydrogen-bonding interactions between cations and anions [N14−H7···N24^{i} 2.854(2); N30−H12···N11^{ii} 2.854(2); N15−H13···N21^{i} 3.057(2); N31−H5···N5^{ii} 3.086(2); N1−H1B···N32 3.096(2); N14−H9···N9^{iii} 3.063(2) Å. Symmetry codes: i: $-x+1$, $-y$, $-z+1$; ii: $x+1$, y, z; iii: $-x+1$, $y-1/2$, $-z+1/2$] and weak hydrogen-bonding interactions from different independent molecules [N1−H1A···O20^{iv} 3.0562(19); N17-H16···O4^{v} 3.029(2); N30−H3···N26^{vi} 3.080(2); N30−H3···N(25)^{vi} 3.089(2) Å. Symmetry codes: iv: x, $-y+3/2$, $z-1/2$; v: $x+1$, $-y+3/2$, $z+1/2$; vi: x, $-y+1/2$, $z-1/2$]. The packing diagram of the structure is shown in Figure 1b. There are no significant interactions between adjacent double layers.

Compound **9** crystallizes in the monoclinic space group *C*2/*c*. As shown in Figure 2a, the asymmetric unit consists of one crystallographically independent AFT anion and one carbonic hydrazylhydrazidinium cation, in which the formation of the monocationic compound is confirmed despite the metathesis reaction being carried out using dicationic carbonic dihydrazidinium sulfate (supra infra). In the AFT anion, the atoms in either the tetrazolate or furazan rings are planar with mean deviations from their respective ring plane of 0.0018 and 0.0004 Å. The exocyclic amine nitrogen atom N1 is out of the furazan plane by 0.0472 Å. The dihedral angle between the tetrazolate and the

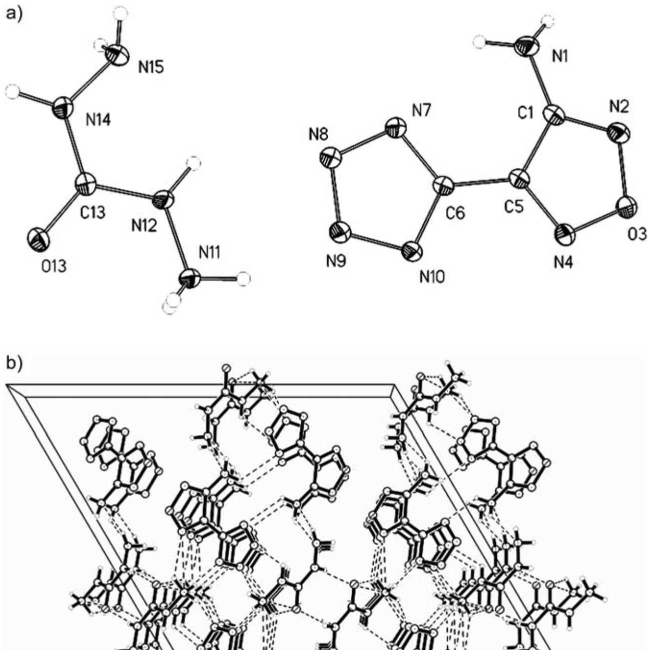

Figure 2. a) Molecular structure of **9** with thermal ellipsoids at 50% probability; b) packing diagram of **9** along the *b* axis.

furazan group is 1.9°. All of these values are comparable with those in **4**. In addition, the bond lengths and bond angles of the AFT anion are close to those in **4**. The atoms of the hydrazylhydrazidinium cation are also planar with mean deviations from the plane being 0.0171 Å. It should be noted that the N14–N15 bond length [1.4150(12) Å] in the cation is very close to that of N11–N12 [1.4119(11) Å]; however, the C13–N14 bond length [1.3398(13) Å] is shorter than that of N12–C13 [1.3617(13) Å]. Interestingly, the cation and anion in **9** are slightly twisted; the dihedral angle between them is 10.5°. In the salts, the amino groups in both the AFT and cation serve as excellent hydrogen-bonding donors and the carbonyl of the cation and the tetrazolate of AFT act as hydrogen-bonding acceptors; thus, extensive hydrogen bonds were formed, which results in the high density of these salts. As shown in Figure 2b, the discrete AFT and hydrazylhydrazidinium are linked into a 3D network by the extensive hydrogen-bonding interactions between cation and anion [N1–H1B···N7 3.0528(13); N11–H11A···N9 2.7638(13); N12–H12A···N8 3.0575(13); N11–H11B···N4^{i} 2.9672(12); N11–H11C···N10^{i} 2.8221(12) Å. Symmetry code: i: $-x$, $y-1$, $-z+1/2$] as well as between cation and cation N11–H11B···O13^{ii} 2.8567(12); [N14–H14A···O13^{iii} 2.9055(12) Å Symmetry codes: ii: x, $y+1$, z; iii: $-x$, $-y+1$, $-z$].

Compound **13** crystallizes in the orthorhombic space group $P2_12_12_1$. As shown in Figure 3a, the asymmetric unit contains one crystallographically independent AFT anion and one 1,4-dimethyl-5-aminotetrazolium cation. In AFT, the atoms in the tetrazolate and the furazan ring are planar with mean deviations from their respective ring plane of 0.0010 and 0.0006 Å. The exocyclic amine nitrogen atom N9 is out of the furazan plane by 0.0228 Å. The dihedral angle between the tetrazolate and the furazan group is 9.4°, which is larger than those in **4** and **9**. The bond lengths and bond angles of the AFT anion are close to those in **4** and **9**. The tetrazolium ring in 1,4-dimethyl-5-aminotetrazolium is also planar with a mean deviation from the plane of 0.0026 Å. The exocyclic nitrogen atom N1 is out of the tetrazolium plane by 0.0401 Å. The dihedral angle between the AFT and the 1,4-dimethyl-5-aminotetrazolium is 19.5°. It should be mentioned that the N4–N5 bond length [1.2751(17) Å] in the tetrazolium ring is shorter than the corresponding N17–N18 bond length in the tetrazolate ring [1.3247(15) Å]; however, the other two N–N bond lengths are inverse [N3–N4 1.3653(16), N5–N6 1.3611(15), N16–N17 1.3448(15), N18–N19 1.3401(16) Å], while their C–N bond lengths are very similar in length. As shown in Figure 3b, the discrete cations and anions are linked into a 3D network by the extensive hydrogen-bonding interactions between AFT and 1,4-dimethyl-5-aminotetrazolium [N1–H1B···N17 2.8779(17); N1–H1A···N18^{i} 2.9129(16) Å. Symmetry code: i: $x+1/2$, $-y+3/2$, $-z+1$] as well as between AFT and AFT [N9–H9A···N19 2.9439(17); N9–H9B···N16^{ii} 3.0850(16) Å. Symmetry code: ii: $-$x, $y+1/2$, $-z+1/2$].

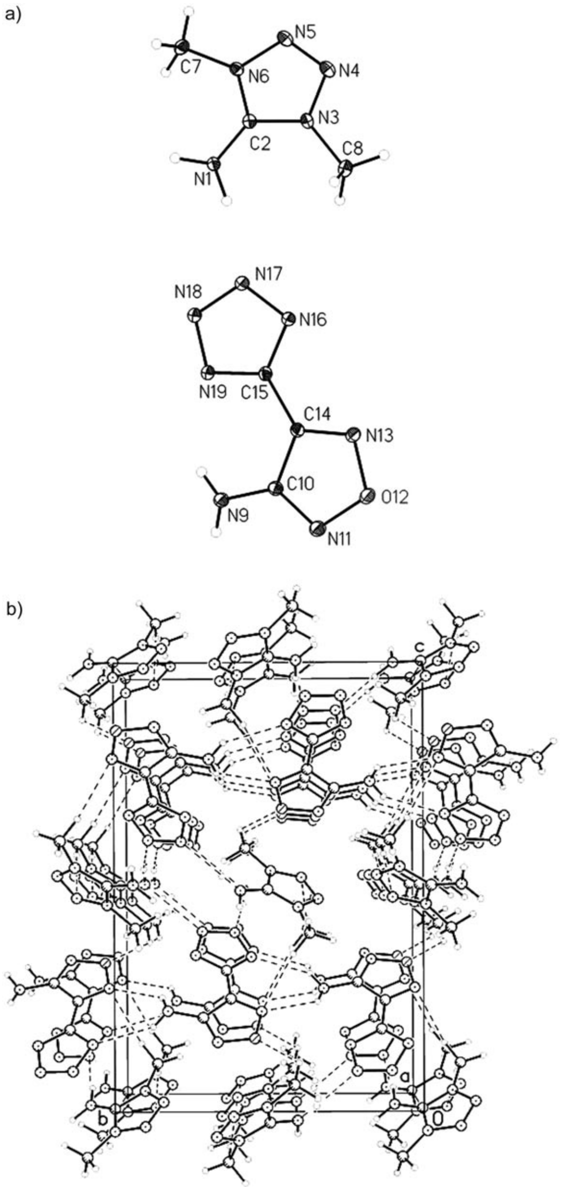

Figure 3. a) Molecular structure of **13** with thermal ellipsoids at 50% probability; b) packing diagram of **13** along the *a* axis.

Conclusions

A series of furazan-functionalized tetrazolate-based energetic salts were synthesized and characterized. Since these salts combine the properties of a furazan fragment and a tetrazolate backbone, they exhibit excellent thermal stability and high positive heats of formation. Aside from salt **12** (170 °C), the degradation temperature of these salts exceeds 190 °C. Most of them are higher than their 5-substituted tetrazolate analogues and other furazan-based salts. The heats of formation of the salts **1**–**13** fall in the range from 177.2 to 730.1 kJ mol^{-1}, which are higher than their 5-nitrotetrazolate, 5-nitraminotetrazolate, and 5-aminotetrazolate analogues. Despite the lower oxygen balance and lower density, the calculated detonation velocity and pressure in some salts are comparable with those of conventional explosives, such as TNT and TATB. Moreover, all of the salts can be classified as insensitive materials.

Experimental Section

Caution: Although we experienced no difficulties in handling these energetic materials, small-scale and best safety practices (leather gloves, face shield) are strongly encouraged!

General methods: 4-Amino-3-(5-tetrazolyl)furazan[19b,c] was prepared as reported previously. IR spectra were recorded with KBr plates using a BIORAD model 3000 FTS spectrometer. ^1H and ^{13}C spectra were recorded on spectrometers at 300 and 75 MHz, respectively, by using $[D_6]$DMSO as a locking solvent. Chemical shifts were reported in ppm relative TMS. Densities were measured at 25 °C using a Micromeritics Accupyc 1330 gas pycnometer. Differential scanning calorimetry (DSC) measurements were performed by using a calorimeter equipped with an auto-cool accessory and calibrated by using indium. The samples were heated from 40 to 400 °C at 10 °C min^{-1}. The transition temperature T_m was taken as the peak maximum. Thermogravimetric analysis (TGA) measurements were carried out by heating samples at 10 °C min^{-1} from 25 to 600 °C in a dynamic nitrogen atmosphere (flow rate = 70 mL min^{-1}). Elemental analyses were performed on a CE-440 Elemental Analyzer.

Theoretical study: Calculations were carried out using the Gaussian 03 (Revision D.01) suite of programs.[25] The geometric optimization of the structures and frequency analyses were carried out using B3-LYP functional with the 6–31+G** basis set, and single-point energies were calculated at the MP_2(full)/6–311++G** level. All of the optimized structures were characterized to be true local energy minima on the potential energy surface without imaginary frequencies.

Based on a Born–Haber energy cycle (Scheme 3), the heat of formation of a salt can be simplified by Equation (1):

$$\Delta H_f^\circ(\text{ionic salt, 298 K}) = \Delta H_f^\circ(\text{cation, 298 K}) + \Delta H_f^\circ(\text{anion, 298 K}) - \Delta H_L \tag{1}$$

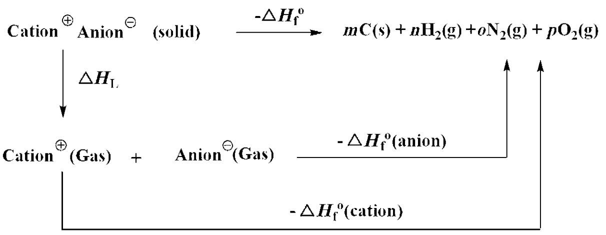

Scheme 3. Born–Haber cycle for the formation of energetic salts

where ΔH_L is the lattice energy of the salt which could be predicted by the formula suggested by Jenkins et al.[26] as given in Equation (2):

$$\Delta H_L = U_{POT} + [p(nM/2-2) + q(n_X/2-2)]RT \tag{2}$$

where nM and n_X depend on the nature of the ions M_p^+ and Xq^-, respectively, and are equal to 3 for monatomic ions, 5 for linear polyatomic ions, and 6 for nonlinear polyatomic ions. The equation for lattice potential energy U_{POT} has the form given in Equation (3),

$$U_{POT}/\text{kJ mol}^{-1} = \gamma(\rho_m/M_m)^{1/3} + \delta \tag{3}$$

where density, ρ_m [g cm^{-3}], M_m is the chemical formula mass of the ionic material (g), and the coefficients γ [kJ mol^{-1} cm] and δ [kJ mol^{-1}] are assigned literature values.[25] The heat of formation of furazan was calculated using G2. The heat of formation of the AFT anion was computed using the method of isodesmic reactions (Scheme 2). The enthalpy of an isodesmic reaction (ΔH_{r298}°) is obtained by combining the MP2(full)/6–311++G** energy difference for the reaction, the scaled zero point energies(B3LYP/6-31+G**), and other thermal factors (B3LYP/6-31+G**).

X-ray crystallography: Crystals of compound **4** and **13** were removed from the flask, a suitable crystal was selected, attached to a glass fiber, and data were collected at 90(2) K using a Bruker/Siemens SMART APEX instrument ($Mo_{K\alpha}$ radiation, $\lambda = 0.71073$ Å) equipped with a Cryocool NeverIce low temperature device. Data were measured by using omega scans of 0.3° per frame for 15 s for **4** and for 10 s for **13**, and a full sphere of data was collected. A total of 2400 frames were collected with a final resolution of 0.77 Å for **4** and 0.71 Å for **13**. Cell parameters were retrieved by using SMART[27] software and refined by using SAINTPlus[28] on all observed reflections. Data reduction and correction for Lp and decay were performed by using the SAINTPlus software. Absorption corrections were applied using SADABS.[29] The structure was solved by direct methods and refined by least-squares methods on F^2 using the SHELXTL program package.[30] The structure was solved in the space group $P2(1)/c$ (no. 14) for **4** and $P2(1)2(1)2(1)$ (no. 19) for **13** by analysis of the systematic absences. All other non-hydrogen atoms were refined anisotropically. Hydrogen atoms were both added geometrically (riding model) and by refinement.

A crystal of compound **9** was mounted on a MiteGen MicroMesh using a small amount of Cargille Immersion Oil. Data were collected on a Bruker three-circle platform diffractometer equipped with a SMART APEX II CCD detector. The crystals were irradiated by using graphite-monochromated $Mo_{K\alpha}$ radiation ($\lambda = 0.71073$). An MSC X-Stream low-temperature device was used to keep the crystals at a constant 140(2) K during data collection. Data collection was performed and the unit cell was initially refined by using APEX2 [v2.1-0].[31] Data reduction was performed by using SAINT [v7.34 A][32] and XPREP [v6.12].[33] Corrections were applied for Lorentz, polarization, and absorption effects using SADABS [v2004/1].[34] The structure was solved and refined with the aid of the programs in the SHELXTL-plus [v6.12] system of programs.[35] The full-matrix least-squares refinement on F^2 included atomic coordinates and anisotropic thermal parameters for all non-H atoms. The H atoms were included by using a riding model.

No decomposition was observed during data collection of crystals **4**, **9**, and **13**. Details of the data collection and refinement are given in Table 3.

CCDC-704938 (**4**), CCDC-704939 (**9**), and CCDC-704940 (**13**) contain the supplementary crystallographic data for this paper. These data can be obtained free of charge from The Cambridge Crystallographic Data Centre via www.ccdc.cam.ac.uk/data_request/cif.

Ammonium 4-amino-3-(5-tetrazolate)furazan (1): A solution of 30 % ammonia (0.113 g, 2.0 mmol) in MeOH (5 mL) was added dropwise to a stirring solution of 4-amino-3-(5-tetrazole)furazan (0.1531 g, 1.0 mmol) in MeOH (30 mL) and the resulting solution was stirred at 25 °C for 6 h. After removal of the solvent in vacuo, the residue was washed twice with Et_2O (10 mL) to give a colorless solid. Yield: 0.15 g (88 %). ^1H NMR: $\delta = 7.13$ (s, 4H), 6.51 ppm (s, 2H); ^{13}C NMR: $\delta = 155.9$, 151.1, 140.4 ppm; IR: $\tilde{\nu} = 3426$ (w), 3321 (w), 3251 (w), 3166 (w), 2991 (w), 2842 (w), 2194 (vw), 1934 (w), 1842 (w), 1699 (m), 1630 (s), 1597 (m), 1567 (w), 1445 (s), 1360 (m), 1213 (vw), 1157 (s), 1084 (vw), 1032 (m), 983 (s), 893 (m), 866 (m), 773 (w), 717 (vw), 619 (m), 483 cm^{-1} (w); elemental analysis (%) calcd for $C_3H_6N_8O$ (170.13): C 21.18, H 3.55, N 65.86; found: C 21.05, H 3.52, N 65.09.

General procedures for the preparation of the energetic compounds 2–9: Barium hydroxide (0.1578 g, 0.5 mmol) was added to a stirring solution of 4-amino-3-(5-tetrazole)furazan (0.1531 g, 1.0 mmol) in H_2O (50 mL) and the resulting mixture was stirred at 25 °C until all of the solids had dissolved, and then the sulfate salt (0.5 mmol) was added and the mixture was stirred at 25 °C for an additional 1 h. After removal of $BaSO_4$, the solvent was evaporated in vacuo, the residue was washed twice with Et_2O (5 mL), and then recrystallized from $EtOH/Et_2O$.

Hydrazinium 4-amino-3-(5-tetrazolate)furazan (2): Colorless solid, yield: 0.15 g (81 %). ^{1}H NMR: $\delta = 6.52$ ppm (s); ^{13}C NMR: $\delta = 155.9$, 151.0, 140.2 ppm; IR: $\tilde{\nu} = 3429$ (w), 3327 (vw), 3167 (vw), 2704 (vw), 2599 (vw), 2214 (vw), 2150 (w), 1954 (w), 1784 (vw), 1633 (s), 1605 (s), 1568 (s), 1508 (m), 1427 (m), 1364 (s), 1242 (w), 1213 (w), 1153 (s), 1109 (s), 1034 (w), 983 (s), 943 (s), 870 (w), 856 (m), 768 (vw), 724 (w), 611 (vw), 563(w), 465 cm^{-1} (w); elemental analysis calcd (%) for $C_3H_7N_9O$ (185.15): C 19.46, H 3.81, N 68.09; found: C 19.44, H 3.70, N 67.29.

Guanidinium 4-amino-3-(5-tetrazolate)furazan (3): Colorless solid, yield: 0.20 g (94 %). ^{1}H NMR: $\delta = 6.94$ (s, 6H), 6.50 (s, 2H); ^{13}C NMR: $\delta = 158.4$, 155.9, 151.0, 140.3 ppm; IR: $\tilde{\nu} = 3599$ (vw), 3493 (w), 3397 (w), 3331 (w), 3211 (w), 3083 (w), 2828 (vw), 2206 (vw), 2142 (vw), 1686 (s), 1642 (s), 1597 (s), 1558 (w), 1430 (m), 1364 (m), 1211 (vw), 1155 (s), 1084 (vw), 1035 (w), 980 (s), 895 (w), 870 (m), 766 (w), 741 (w), 662 (vw), 567 (w), 516 cm^{-1} (w); elemental analysis calcd (%) for $C_4H_8N_{10}O$ (212.17): C 22.64, H 3.80, N 66.02; found: C 22.52, H 3.81, N 64.75.

Aminoguanidinium 4-amino-3-(5-tetrazolate)furazan (4): Colorless solid, yield: 0.18 g (79 %). ^{1}H NMR: $\delta = 8.52$ (d, $J = 7.7$ Hz, 1H), 6.92 (s, 2H), 6.73 (s, 2H), 6.51 (s, 2H), 4.65 ppm (s, 2H); ^{13}C NMR: $\delta = 159.3$, 155.9, 151.1, 140.4 ppm; IR: $\tilde{\nu} = 3489$ (w), 3429 (w), 3377 (w), 3269 (w), 3192 (vw), 3039 (w), 2883 (vw), 2755 (w), 2195 (vw), 1842 (w), 1665 (s), 1630 (s), 1599 (m), 1566 (m), 1443 (m), 1430 (m), 1362 (m), 1213 (vw), 1152 (m), 1101 (w), 1042 (vw), 988 (s), 904 (w), 864 (m), 773 (vw), 741 (vw), 676 (m), 565 (w), 513 cm^{-1} (vw); elemental analysis calcd (%) for $C_4H_9N_{11}O$ (227.19): C 21.15, H 3.99, N 67.82; found: C 21.15, H 3.91, N 67.38.

Diaminoguanidinium 4-amino-3-(5-tetrazolate)furazan (5): Colorless solid, yield: 0.21 g (87 %). ^{1}H NMR: $\delta = 8.56$ (s, 2H), 7.14 (s, 2H), 6.51 (s, 2H), 4.58 (s, 4H); ^{13}C NMR: $\delta = 160.3$, 155.9, 151.1, 140.4 ppm; IR: $\tilde{\nu} = 3455$ (w), 3349 (w), 3273 (w), 3204 (w), 3144 (vw), 2983 (vw), 2363 (vw), 1954 (vw), 1682 (s), 1630 (s), 1593 (s), 1482 (vw), 1422 (w), 1356 (m), 1213 (m), 1180 (m), 1155 (s), 1123 (w), 1013 (s), 976 (m), 864 (m), 756 (w), 679 (m), 565 cm^{-1} (m); elemental analysis calcd (%) for $C_4H_{10}N_{12}O$ (242.20): C 19.84, H 4.16, N 69.40; found: C 19.86, H 4.14, N 68.92.

Triaminoguanidinium 4-amino-3-(5-tetrazolate)furazan (6): Colorless solid, yield: 0.19 g (74 %). ^{1}H NMR: $\delta = 8.57$ (s, 3H), 6.52 (s, 2H), 4.47 ppm (s, 6H); ^{13}C NMR: $\delta = 159.5$, 155.9, 151.1, 140.4 ppm; IR: $\tilde{\nu} = 3424$ (w), 3379 (w), 3331 (w), 3179 (vw), 2797 (vw), 2497 (vw), 2195 (vw), 1937 (w), 1844 (vw), 1686 (s), 1634 (s), 1600 (m), 1572 (m), 1444 (w), 1427 (m), 1358 (s), 1211 (vw), 1198 (m), 1138 (s), 1033 (vw), 978 (s), 900 (w), 864 (m), 770 (vw), 730 (vw), 649 (w), 624 (vw), 505 cm^{-1} (w); elemental analysis calcd (%) for $C_4H_{11}N_{13}O$ (257.22): C 18.68, H 4.31, N 70.79; found: C 18.52, H 4.26, N 70.03.

***N*-carbamoylguanidinium 4-amino-3-(5-tetrazolate)furazan hydrate (7)**: Colorless solid, yield: 0.17 g (62 %). ^{1}H NMR: $\delta = 8.04$ (s, 4H), 7.11 (s, 2H), 6.51 ppm (s, 2H); ^{13}C NMR: $\delta = 155.9$, 154.8, 151.0, 140.4 ppm; IR: $\tilde{\nu} = 3376$ (w), 3198 (w), 2806 (w), 2211 (vw), 2144 (vw), 1731 (s), 1699 (s), 1624 (s), 1593 (m), 1572 (w), 1466 (m), 1432 (vw), 1383 (m), 1364 (s), 1215 (w), 1157 (m), 1127 (m), 1092 (w), 1035 (vw), 920 (w), 882 (m), 760 (m), 708 (w), 604 (w), 443 cm^{-1} (w); elemental analysis calcd (%) for $C_5H_9N_{11}O_2 \cdot H_2O$ (273.21): C 21.98, H 4.06, N 56.39; found: C 21.62, H 3.89, N 55.05.

Guanidylguanidinium 4-amino-3-(5-tetrazolate)furazan (8): Colorless solid, yield: 0.13 g (51 %). ^{1}H NMR: $\delta = 6.77$ (s, 3H), 6.50 ppm (s, 2H); ^{13}C NMR: $\delta = 160.2$, 155.9, 152.0, 151.1, 140.4 ppm; IR: $\tilde{\nu} = 3464$ (w), 3426 (w), 3352 (w), 3238 (vw), 3171 (vw), 2778 (vw), 2127 (w), 1663 (s), 1629 (s), 1602 (w), 1591(s), 1586 (s), 1427 (w), 1363 (m), 1214 (w), 1155 (m), 1034 (vw), 990 (m), 904 (w), 868 (vw), 771 (w), 732 (w), 590 (w), 510 (w), 455 cm^{-1} (w); elemental analysis calcd (%) for $C_5H_{10}N_{12}O$ (254.21): C 23.62, H 3.96, N 66.12; found: C 23.65, H 3.90, N 65.51.

Carbonic hydrazylhydrazidinium 4-amino-3-(5-tetrazolate)furazan (9): Pale yellow solid, yield: 0.11 g (45 %). ^{1}H NMR: $\delta = 6.52$ (s, 2H), 3.41 (quart, $J = 7.0$, 14.0 Hz, 2H) 1.03 ppm (t, $J = 7.0$ Hz, 3H); ^{13}C NMR: $\delta = 159.4$, 155.9, 151.1, 140.4 ppm; IR: $\tilde{\nu} = 3442$ (w), 3343 (m), 3240 (w), 3172 (vw), 2854 (w), 2625 (w), 1982 (w), 1868 (vw), 1701 (m), 1630 (s), 1595 (s), 1586 (m), 1504 (m), 1447 (w), 1432 (w), 1354 (m), 1246 (w), 1207 (w), 1190 (vw), 1153 (s), 1113 (w), 1007 (s), 984 (s), 908 (w), 878 (w), 735 (vw), 680 (vw), 580 (w), 542 (w), 501 cm^{-1} (w); elemental analysis calcd (%) for $C_4H_9N_{11}O_2$ (243.19): C 19.76, H 3.73, N 63.36; found: C 19.78, H 3.66, N 62.55.

1-Methylimidazolium 4-amino-3-(5-tetrazolate)furazan (10): 1-Methylimidazole (0.246 g, 3.0 mmol) was added to a stirring solution of 4-amino-3-(5-tetrazole) furazan (0.306 g, 2.0 mmol) in MeOH (30 mL) and the resulting solution was stirred at 60 °C for 24 h. After removal of the solvent in vacuo, the residue was washed four times with Et_2O (20 mL) to give a colorless solid. Yield: 0.18 g (31 %). ^{1}H NMR: $\delta = 8.93$ (s, 1H), 7.62 (s, 1H), 7.58 (s, 1H), 6.51 ppm (s, 2H); ^{13}C NMR: $\delta = 170.0$, 155.9, 140.2, 136.4, 123.5, 120.8 ppm; IR: $\tilde{\nu} = 3463$ (w), 3357 (m), 3134 (m), 3071 (w), 2974 (vw), 2726 (vw), 2479 (vw), 1939 (vw), 1762 (vw), 1630 (vs), 1589 (s), 1555 (m), 1477 (vw), 1452 (vw), 1420 (w), 1366 (m), 1335 (w), 1275 (m), 1194 (w), 1149 (w), 1090 (m), 1013 (vw), 977 (s), 883 (m), 853 (m), 761 (s), 730 (vw), 629 (m), 567 (w), 507 cm^{-1} (w); elemental analysis calcd (%) for $C_7H_9N_9O$ (235.21): C 35.75, H 3.86, N 53.60; found: C 35.52, H 3.79, N 52.45.

General procedures for the preparation of the energetic compounds 11–13: Barium hydroxide (0.1578 g, 0.5 mmol) was added to a stirring solution of 4-amino-3-(5-tetrazole)furazan (0.1531 g, 1.0 mmol) in H_2O (30 mL) and the resulting mixture was stirred at 25 °C until all of solids had dissolved. This solution was added to a stirring mixture of Ag_2SO_4 (0.1559 g, 0.5 mmol) and iodide salts (0.5 mmol) in H_2O (30 mL). The resulting mixture was stirred at 25 °C for 0.5 h. After the mixture had been filtered, slow evaporation the of filtrate gave rise to desirable products, which were washed twice with Et_2O.

1,4-Dimethyltriazolium 4-amino-3-(5-tetrazolate)furazan hemihydrate (11): Colorless solid, yield: 0.16 g (62 %). ^{1}H NMR: $\delta = 9.96$ (s, 1H), 9.07 (s, 1H), 6.52 (s, 2H), 4.04 (s, 3H), 3.87 ppm (s, 3H); ^{13}C NMR: $\delta = 155.9$, 151.1, 145.8, 143.9, 140.4, 39.0, 34.4 ppm; IR: $\tilde{\nu} = 3513$ (vw), 3383 (vw), 3279 (vw), 3148 (vw), 2497 (vw), 2212 (vw), 2112 (vw), 1967 (vw), 1798 (w), 1633 (s), 1589 (s), 1569 (s), 1437 (m), 1429 (s), 1360 (s), 1292 (vw), 1234 (vw), 1205 (m), 1153 (s), 1098 (vw), 1071 (m), 1028 (m), 981 (s), 909 (m), 869 (m), 771 (vw), 732 (m), 660 (vw), 621 (w), 569 (w), 525 cm^{-1} (w); elemental analysis calcd (%) for $C_7H_{10}N_{10}O \cdot 0.5H_2O$ (259.23): C 32.43, H 4.28, N 54.03; found: C 32.19, H 4.10, N 53.85.

1,4,5-Trimethyltetrazolium 4-amino-3-(5-tetrazolate)furazan (12): Colorless solid, yield: 0.20 g (75 %). ^{1}H NMR: $\delta = 6.51$ (s, 2H), 4.21 (s, 6H), 2.83 ppm (s, 3H); ^{13}C NMR: $\delta = 155.9$, 153.2, 151.0, 140.4, 36.7, 8.7 ppm; IR: $\tilde{\nu} = 3422$ (w), 3393 (w), 3283 (vw), 3150 (w), 3040 (vw), 2293 (vw), 2094 (vw), 1634 (s), 1586 (m), 1566 (m), 1534 (w), 1443 (m), 1427 (w), 1358 (s), 1329 (w), 1242 (vw), 1201 (m), 1144 (s), 1036 (m), 981 (s), 879 (m), 847 (m), 757 (m), 729 (w), 691 (vw), 663 (vw), 563 (m), 507 cm^{-1} (vw); elemental analysis calcd (%) for $C_7H_{11}N_{11}O$ (265.24): C 31.70, H 4.18, N 58.09; found: C 31.62, H 4.14, N 57.46.

1,4-Dimethyl-5-aminotetrazolium 4-amino-3-(5-tetrazolate)furazan (13): Pale yellow solid, yield: 0.24 g (90 %). ^{1}H NMR: $\delta = 6.51$ (s, 2H), 3.84 ppm (s, 6H); ^{13}C NMR: $\delta = 158.6$, 155.9, 149.0, 140.3, 43.0, 34.4 ppm; IR: $\tilde{\nu} = 3441$ (w), 3339 (w), 3256 (w), 3136 (w), 2943 (w), 2887 (vw), 2698 (vw), 2486 (vw), 2219 (vw), 2145 (vw), 1699 (s), 1654 (m), 1626 (s), 1599 (m), 1563 (w), 1541 (w), 1451 (m), 1413 (m), 1392 (vw), 1352 (m), 1201 (m), 1146 (s), 1106 (vw), 1067 (w), 1028 (m), 985 (s), 895 (w), 858 (w), 782 (m), 731 (w), 675 (w), 575 (vw), 496 cm^{-1} (vw); elemental analysis calcd (%) for $C_6H_{10}N_{12}O$ (266.22): C 27.07, H 3.79, N 63.14; found: C 26.75, H 3.79, N 62.20.

Acknowledgements

The financial support of the DTRA (HDTRA1–07–1–0024), NSF (Grant CHE0315275), and ONR (Grant N00014–06–1–1032) is gratefully acknowledged. The Bruker (Siemens) SMART APEX diffraction facility was established at the University of Idaho with the assistance of the NSF-EPSCoR program and the M. J. Murdock Charitable Trust, Vancouver, WA, USA.

---

[1] a) J. P. Agrawal, *Prog. Energy Combust. Sci.* **1998**, *24*, 1–30; b) D. E. Chavez, M. A. Hiskey, R. D. Gilardi, *Angew. Chem.* **2000**, *112*, 1861–1863; *Angew. Chem. Int. Ed.* **2000**, *39*, 1791–1793; c) M. H. V. Huynh, M. A. Hiskey, D. E. Chavez, D. L. Naud, R. D. Gilardi, *J. Am. Chem. Soc.* **2005**, *127*, 12537–12543; d) M. Smiglak, A. Metlen, R. D. Rogers, *Acc. Chem. Res.* **2007**, *40*, 1182–1192; e) R. P. Singh, R. D. Verma, D. T. Meshri, J. M. Shreeve, *Angew. Chem.* **2006**, *118*, 3664–3682; *Angew. Chem. Int. Ed.* **2006**, *45*, 3584–3601.

[2] a) L. E. Fried, M. R. Manaa, P. F. Pagoria, R. L. Simpson, *Annu. Rev. Mater. Res.* **2001**, *31*, 291–321; b) M. W. Schmidt, M. S. Gordon, J. A. Boatz, *J. Phys. Chem. A* **2005**, *109*, 7285–7295; c) C. B. Jones, R. Haiges, T. Schroer, K. O. Christe, *Angew. Chem.* **2006**, *118*, 5103–5106; *Angew. Chem. Int. Ed.* **2006**, *45*, 4981–4984.

[3] a) A. K. Zelenin, M. L. Trudell, R. D. Gilardi, *J. Heterocycl. Chem.* **1998**, *35*, 151–155; b) A. B. Sheremetev, N. S. Aleksandrova, *Russ. Chem. Bull.* **2005**, *54*, 1715–1719.

[4] a) A. B. Sheremetev, V. O. Kulagina, N. S. Aleksandrova, D. E. Dmitriev, Y. A. Strelenko, V. P. Lebedev, Y. N. Matyushin, *Propellants Explos. Pyrotech.*, **1998**, *23*, 142–149; b) S. D. Shaposhnikov, N. V. Korobov, A. V. Sergievskii, S. V. Pirogov, S. F. Mel′nikova, I. V. Tselinskii, *Russ. J. Org. Chem.* **2002**, *38*, 1351–1355.

[5] A. V. Sergievskii, T. V. Romanova, S. F. Mel′nikova, I. V. Yselinskii, *Russ. J. Org. Chem.* **2005**, *41*, 261–267.

[6] A. B. Sheremetev, I. L. Yudin, *Mendeleev Commun.* **2002**, *12*, 66–67.

[7] a) Z. X. Li, S. Q. Tang, Y. X. Ou, B. R. Chen, *J. Energ. Mater.* **2002**, *10*, 59–65; b) X. G. Zhang, H. Zhu, W. Zhang, J. Q. Zhang, S. Q. Yang, *Chem. Prop. Poly. Mater.* **2006**, *3*, 1–5.

[8] a) S. D. Shaposhnikov, N. V. Korobov, A. V. Sergievskii, S. V. Pirogov, S. F. Mel′nikova, I. V. Tselinskii, *Russ. J. Org. Chem.* **2002**, *38*, 1351–1355; b) J. C. Bottaro, M. A. Petrie, P. E. Penwell, D. C. Bomberger, *PCT Int. Appl.* **2003**; WO0306371A1; c) P. H. Olesen, A. R. Sørebsen, B. Ursø, P. Kurtzhals, A. N. Bowler, U. Ehrbar, B. F. Hansen, *J. Med. Chem.* **2003**, *46*, 3333–3341; d) J. H. Come, J. Green, C. Marhefka, S. L. Harbeson, L. Pham, US 7157476 B2, **2007**.

[9] a) G. W. Drake, T. Hawkins, A. Brand, L. Hall, M. Mckay, *Propellants Explos. Pyrotech.* **2003**, *28*, 174–180; b) G. W. Drake, T. W. Hawkins, L. A. Hall, J. A. Boatz, A. J. Brand, *Propellants Explos. Pyrotech.* **2005**, *30*, 329–337.

[10] a) A. R. Katritzky, S. Singh, K. Kirichenko, J. D. Holbrey, M. Smiglak, W. M. Reichert, R. D. Rogers, *Chem. Commun.* **2005**, 868–870; b) A. R. Katritzky, H. Yang, D. Zhang, K. Kirichenko, M. Smiglak, J. D. Holbrey, W. M. Reichert, R. D. Rogers, *New J. Chem.* **2006**, *30*, 349–358; c) A. R. Katritzky, S. Singh, K. Kirichenko, M. Smiglak, J. D. Holbrey, W. M. Reichert, S. K. Spear, R. D. Rogers, *Chem. Eur. J.* **2006**, *12*, 4630–4641.

[11] a) C. Ye, H. Gao, J. A. Boatz, G. W. Drake, B. Twamley, J. M. Shreeve, *Angew. Chem.* **2006**, *118*, 7420–7423; *Angew. Chem. Int. Ed.* **2006**, *45*, 7262–7265; b) H. Gao, C. Ye, O. D. Gupta, J. C. Xiao, M. A. Hiskey, B. Twamley, J. M. Shreeve, *Chem. Eur. J.* **2007**, *13*, 3853–3860; c) R. Wang, H. Gao, C. Ye, J. M. Shreeve, *Chem. Mater.* **2007**, *19*, 144–152; d) Y. H. Joo, B. Twamley, S. Garg, J. M. Shreeve, *Angew. Chem.* **2008**, *120*, 6332–6335; *Angew. Chem. Int. Ed.* **2008**, *47*, 6236–6239; e) T. Abe, G. H. Tao, Y. H. Joo, Y. Huang, B. Twamley, J. M. Shreeve, *Angew. Chem.* **2008**, *120*, 7195–7198; *Angew. Chem. Int. Ed.* **2008**, *47*, 7087–7090.

[12] a) H. Xue, B. Twamley, J. M. Shreeve, *Adv. Mater.* **2005**, *17*, 2142–2146; b) C. F. Ye, J. C. Xiao, B. Twamley, J. M. Shreeve, *Chem. Commun.* **2005**, 2750–2752; c) C. M. Jin, C. F. Ye, C. Piekarski, B. Twamley, J. M. Shreeve, *Eur. J. Inorg. Chem.* **2005**, 3760–3767; d) Y. Guo, H. Gao, B. Twamley, J. M. Shreeve, *Adv. Mater.* **2007**, *19*, 2884–2888; e) R. Wang, H. Gao, C. Ye, B. Twamley, J. M. Shreeve, *Inorg. Chem.* **2007**, *46*, 932–938; f) Z. Zeng, H. Gao, B. Twamley, J. M. Shreeve, *J. Mater. Chem.* **2007**, *17*, 3819–3826; g) H. Xue, H. Gao, B. Twamley, J. M. Shreeve, *Chem. Mater.* **2007**, *19*, 1731–1739; h) H. Gao, Y. Huang, C. Ye, B. Twamley, J. M. Shreeve, *Chem. Eur. J.* **2008**, *14*, 5596–5603.

[13] a) T. M. Klapötke, P. Mayer, A. Schulz, J. J. Weigand, *J. Am. Chem. Soc.* **2005**, *127*, 2032–2033; b) G. Steinhauser, T. M. Klapötke, *Angew. Chem.* **2008**, *120*, 3376–3394; *Angew. Chem. Int. Ed.* **2008**, *47*, 3330–3347; c) C. Darwich, T. M. Klapötke, C. MiróSabaté, *Chem. Eur. J.* **2008**, *14*, 5756–5771.

[14] a) J. C. Gálvez-Ruiz, G. Holl, K. Karaghiosoff, T. M. Klapötke, K. Löhnwitz, P. Mayer, H. Nöth, K. Polborn, C. J. Rohbogner, M. Suter, J. J. Weigand, *Inorg. Chem.* **2005**, *44*, 4237–4253; b) K. Konstantin, T. M. Klapötke, P. Mayer, H. Piotrowski, K. Polborn, R. L. Willer, J. J. Weigand, *J. Org. Chem.* **2006**, *71*, 1295–1305; c) T. M. Klapötke, K. Karaghiosoff, P. Mayer, A. Penger, J. M. Welch, *Propellants, Propellants Explos. Pyrotech.* **2006**, *31*, 188–195; d) T. M. Klapötke, J. Stierstorfer, *Helv. Chim. Acta* **2007**, *90*, 2132–2150; e) T. M. Klapötke, P. Mayer, C. MiróSabaté, J. M. Welch, N. Wiegand, *Inorg. Chem.* **2008**, *47*, 6014–6027; f) K. Karaghiosoff, T. M. Klapötke, P. Mayer, C. MiróSabaté, A. Penger, J. M. Welch, *Inorg. Chem.* **2008**, *47*, 1007–1019; g) T. M. Klapötke, C. MiróSabaté, *Chem. Mater.* **2008**, *20*, 3629–3637; h) T. M. Klapötke, J. Stierstorfer, A. U. Wallek, *Chem. Mater.* **2008**, *20*, 4519–4530; i) T. M. Klapötke, C. MiróSabaté, *Chem. Mater.* **2008**, *20*, 1750–1763.

[15] a) C. E. Stoner, Jr., A. L. Rheingold, T. B. Brill, *Inorg. Chem.* **1991**, *30*, 360–364; b) A. B. Sheremetev, V. O. Kulagina, I. A. Kryazhevskikh, T. M. Melnikova, N. S. Aleksandrova, *Russ. Chem. Bull.* **2002**, *51*, 1533–1539; c) M. B. Talawar, R. Sivabalan, N. Senthilkumar, G. Prabhu, S. N. Asthana, *J. Hazardous Mater. A* **2004**, *113*, 11–25.

[16] R. L. Willer, R. S. Day, D. J. Park, US 5460669, **1995**.

[17] S. D. Shaposhnikov, T. V. Romanova, N. P. Spiridonova, S. F. Mel′nikova, I. V. Tselinskii, *Russ. J. Org. Chem.* **2004**, *40*, 884–888.

[18] C. Zhang, *J. Mol. Struct.* **2006**, *765*, 77–83, and references therein.

[19] a) T. Ichikawa, T. Kato, T. Takenishi, *J. Heterocycl. Chem.* **1965**, *2*, 253–255; b) V. G. Andrianov, A. V. Eremeev, *Khimiya Geterotsiklicheskikh Soedinenii* **1994**, 693–696; c) J. H. Come, J. Green, C. Marhefka, S. L. Harbeson, L. Pham, *PCT Int. Appl.* **2005**, WO 2005019190.

[20] K. R. Seddon, *J. Chem. Technol. Biotechnol.* *68*, 351–356.

[21] a) C. Ye, J. M. Shreeve, *J. Phys. Chem. A* **2007**, *111*, 1456–1461; b) C. Ye, J. M. Shreeve, *J. Chem. Eng. Data* **2008**, *53*, 520–524.

[22] S. Schneider, T. Hawkins, M. Rosander, G. Vaghjiani, S. Chambreau, G. Drake, *Energy Fuels* **2008**, *22*, 2871–2872.

[23] a) M. W. Schmidt, M. S. Gordon, J. A. Boatz, *J. Phys. Chem. A* **2005**, *109*, 7285–7295; b) K. E. Gutowski, J. D. Holbrey, R. D. Rogers, D. A. Dixon *J. Phys. Chem. B* **2005**, *109*, 23196–23208; c) K. E. Gutowski, R. D. Rogers, D. A. Dixon, *J. Phys. Chem. B* **2007**, *111*, 4788–4800; d) H. Gao, C. Ye, C. Piekarski, J. M. Shreeve *J. Phys. Chem. C.* **2007**, *111*, 10718–10731.

[24] a) L. E. Fried, K. R. Glaesemann and W. M. Howard, P. C. Souers, CHEETAH 5.0 User's Manual., Lawrence Livermore National Laboratory, **2007**; b) J. P. Lu, *Evaluation of the Thermochemical Code -CHEETAH 2.0 for Modelling Explosives Performance*, Edinburgh, **2001**.

[25] Gaussian 03, Revision D.01, M. J. Frisch, G. W. Trucks, H. B. Schlegel, G. E. Scuseria, M. A. Robb, J. R. Cheeseman, J. A. Montgomery, Jr., T. Vreven, K. N. Kudin, J. C. Burant, J. M. Millam, S. S. Iyengar, J. Tomasi, V. Barone, B. Mennucci, M. Cossi, G. Scalmani, N. Rega, G. A. Petersson, H. Nakatsuji, M. Hada, M. Ehara, K. Toyota, R. Fukuda, J. Hasegawa, M. Ishida, T. Nakajima, Y. Honda, O. Kitao, H. Nakai, M. Klene, X. Li, J. E. Knox, H. P. Hratchian, J. B. Cross, V. Bakken, C. Adamo, J. Jaramillo, R. Gomperts, R. E. Stratmann, O. Yazyev, A. J. Austin, R. Cammi, C. Pomelli, J. W. Ochterski, P. Y. Ayala, K. Morokuma, G. A. Voth, P. Salvador, J. J. Dannenberg, V. G. Zakrzewski, S. Dapprich, A. D. Daniels, M. C. Strain, O. Farkas, D. K. Malick, A. D. Rabuck, K. Raghavachari, J. B. Foresman, J. V. Ortiz, Q. Cui, A. G. Baboul, S. Clifford, J. Cioslowski, B. B. Stefanov, G. Liu, A. Liashenko, P. Piskorz, I. Komaromi, R. L. Martin, D. J. Fox, T. Keith, M. A. Al-Laham, C. Y. Peng, A. Nanayakkara, M. Challacombe, P. M. W. Gill, B. Johnson, W. Chen, M. W. Wong, C. Gonzalez, J. A. Pople, Gaussian, Inc., Wallingford CT, **2004**.

[26] H. D. B. Jenkins, D. Tudeal, L. Glasser, *Inorg. Chem.* **2002**, *41*, 2364–2367.
[27] SMART: V.5.626, Bruker Molecular Analysis Research Tool, Bruker AXS, Madison, **2002**.
[28] SAINTPlus: V. 6.45a, Data Reduction and Correction Program, Bruker AXS, Madison, **2003**.
[29] SADABS: V.2.01, an empirical absorption correction program, Bruker AXS Inc., Madison, **2004**.
[30] G. M. Sheldrick, SHELXTL: V. 6.10, Structure Determination Software Suite, Bruker AXS Inc., Madison, **2001**.
[31] Bruker, APEX2 v2.1-0. Bruker AXS Inc., Madison, **2006**
[32] Bruker, SAINT v7.34A. Bruker AXS Inc., Madison, **2005**.
[33] Bruker, SADABS v2004/1, Bruker AXS Inc., Madison, **2004**.
[34] Bruker, XPREP v6.12. Bruker AXS Inc., Madison, **2001**.
[35] Bruker, SHELXTL v6.12. Bruker AXS Inc., Madison, **2000**.

Received: October 31, 2008